Available online at www.sciencedirect.com
ScienceDirect
Bioorganic & Medicinal Chemistry 15 (2007) 4818–4828
Bioorganic & Medicinal Chemistry

Novel isomarabarican triterpenes, exhibiting selective anti-proliferative activity against vascular endothelial cells, from marine sponge *Rhabdastrella globostellata*

Shunji Aoki,[a] Mami Sanagawa,[a] Yasuo Watanabe,[a] Andi Setiawan,[b] Masayoshi Arai[a] and Motomasa Kobayashi[a,*]

[a]*Graduate School of Pharmaceutical Sciences, Osaka University, Yamada-oka 1-6, Suita, Osaka 565-0871, Japan*
[b]*Department of Chemistry, Faculty of Science, Lampung University, Jl. Prof. Dr. Sumantri Brodjonegoro No. 1, Bandar Lampung 35145, Indonesia*

Received 3 April 2007; revised 27 April 2007; accepted 28 April 2007
Available online 6 May 2007

Abstract—Four novel globostellatic acid X methyl esters (**1**–**4**) having isomarabarican-type triterpenoidal skeleton and three related new compounds (**5**–**7**) were isolated from the marine sponge *Rhabdastrella globostellata*, as selective anti-proliferative agents against human umbilical vein endothelial cells (HUVECs). Those chemical structures were elucidated by the detailed 2D NMR analysis. Two globostellatic acid X methyl esters (**3** and **4**) having 13*E*-geometry were found to inhibit proliferation of HUVECs, 80- to 250-fold selectively in comparison with several other cell lines. 13*E*,17*E*-Globostellatic acid X methyl ester (**4**) also inhibited bFGF-induced tubular formation and VEGF-induced migration of HUVECs. Moreover, **4** induced apoptosis of HUVECs, whereas it exhibited no effect on VEGF-induced phosphorylation of ERK1/2 in HUVECs.

1. Introduction

Angiogenesis is a crucial process in normal physiology, while uncontrolled angiogenesis is pathological and is often associated with several diseases such as atherosclerosis, arthritis, diabetic retinopathy, and cancer.[1] Tumor angiogenesis involves several steps including degradation of extracellular matrix by metalloproteinases, proliferation, migration, and tubular formation of endothelial cells. Each of these steps was tightly regulated by angiogenic factors such as vascular endothelial growth factor (VEGF), basic fibroblast growth factor (bFGF), and so on.[2] It has been shown that growth of solid tumor required a corresponding increase in vascularization.[3] We recently isolated bastadin 6, a cyclic tetramer of brominated-tyrosine derivative, from a marine sponge. Bastadin 6 inhibited the proliferation of human umbilical vein endothelial cells (HUVECs) with 20- to 100-fold selectivity in comparison with normal fibroblast or several tumor cell lines. Moreover, bastadin 6 completely blocked the VEGF- or bFGF-induced in vivo neovascularization in the mice corneal assay and suppressed the growth of s.c. inoculated A431 solid tumor in nude mice.[4]

In the course of our search for anti-angiogenic substances from marine organisms, globostellatic acid X methyl esters (**1**–**4**), novel isomarabarican-type triterpenes, and several related compounds were isolated from a marine sponge, as selective anti-proliferative agents against HUVECs. In this paper, the structure elucidation of these compounds and the in vitro anti-angiogenic effects of globostellatic acid X methyl esters are presented.

2. Structure elucidation

The dried marine sponge of *Rhabdastrella globostellata*, which was collected in Indonesia, was extracted with MeOH. The MeOH extract, which showed the selective growth inhibitory activity against HUVECs, was partitioned into *n*-hexane-90% MeOH mixture. On the guidance of bioassay, the *n*-hexane extract was separated by

Keywords: Globostellatic acid X methyl esters; Marine sponge; Anti-angiogenic effect; HUVECs; Tubular formation; Migration.
* Corresponding author. Tel.: +81 66879 8215; fax: +81 66879 8219; e-mail: kobayasi@phs.osaka-u.ac.jp

0968-0896/$ - see front matter © 2007 Elsevier Ltd. All rights reserved.
doi:10.1016/j.bmc.2007.04.070

SiO_2 column and HPLC to provide an active fraction, which was inseparable isomeric mixture having carboxylic acid group. Then, the active fraction was converted into its methyl esters with TMS–diazomethane treatment and separated by reversed-phase HPLC to afford four compounds named 13*Z*,17*Z*-globostellatic acid X methyl ester (**1**), 13*Z*,17*E*-globostellatic acid X methyl ester (**2**), 13*E*,17*Z*-globostellatic acid X methyl ester (**3**), and 13*E*,17*E*-globostellatic acid X methyl ester (**4**). A related compound named acetyljaspiferal E (**7**) was also isolated from the *n*-hexane extract by the similar procedure (Fig. 1).

To obtain structurally related compounds with globostellatic acid X methyl esters for structure–activity relationship study, the 90% MeOH extract was separated by SiO_2 column chromatography. Each fraction was treated with TMS–diazomethane and then purified by reversed-phase HPLC to isolate two new compounds named globostellatic acid F methyl ester (**5**) and 13*E*-globostellatic acid B methyl ester (**6**) together with a known compound, 3-*O*-acetyljaspiferal B methyl ester (**8**)[5] (Fig. 1).

13*E*,17*E*-Globostellatic acid X methyl ester (**4**) was obtained as a bright yellow amorphous powder. The ESI-TOF MS of **4** showed a quasi-molecular ion peak at *m*/*z* 545 $[M+Na]^+$, and the molecular formula was determined as $C_{33}H_{46}O_5$ by high-resolution (HR-) ESI-TOF MS and NMR analysis. The IR absorptions at 1740, 1691, and 1639 cm^{-1} of **4** suggested the presence of ester carbonyl and conjugated ketone groups. The ^1H and ^{13}C NMR data of **4** showed the presence of six olefinic protons, five double bonds, nine methyls, an oxymethine proton, two ester carbonyls, and a keto carbonyl. The UV absorption at 400 nm of **4** indicated the presence of long conjugated olefinic chromophore. Five partial structures (A–E) in **4** were revealed by COSY and HMQC analysis (Fig. 2). The connectivity of these partial structures was figured out on the basis of the HMBC correlations as shown in Figure 2. All the geometries of the olefins in the side chain were determined as *E* by the NOESY correlations between H-15 and H-17, H-30; H-16 and H-18, H-21; H-22 and H-17, H-24; H-23 and H-21, H-26 (Fig. 3) and the coupling constants ($^3J_{15,16}$ = 15.1 Hz, $^3J_{22,23}$ = 15.1 Hz). All the proton- and carbon-signals were assigned as shown in Tables 1 and 2, and the planar structure of **4** was elucidated as shown in Figure 1.

The relative stereostructure of **4** was revealed by the NOESY correlations between H-19 and H-9, methoxycarbonyl-H; H-5 and H-28, H-30; H-7 and H-9. These NOESY correlations also indicated that the A/B ring in **4** has chair/twist-boat conformation (Fig. 3). The coupling constants (J = 2.2 Hz, 2.7 Hz) of the oxymethine proton with the methylene protons at C-2 defined that the acetoxyl group at C-3 has α-axial configuration. These data clarified that compound **4** was isomarabarican-type triterpene as shown in Figure 3. So far, several isomarabarican-type triterpenes having the same *trans–syn–trans* ring-system with **4** (e.g., stellettins[6,7], aurorals[8], rhabdastrellic acid A[9], stelliferins[10], globostellatic acids[11], and jaspiferals[12]) have been isolated from marine sponges of *Rhabdastrella* sp., *Jaspis* sp., and *Stelletta* sp., and the absolute structures for some of them have been elucidated.

The ESI-TOF MS of 13*Z*,17*Z*-globostellatic acid X methyl ester (**1**), 13*Z*,17*E*-globostellatic acid X methyl ester (**2**), and 13*E*,17*Z*-globostellatic acid X methyl ester (**3**) showed the same quasi-molecular ion peak at *m*/*z* 545 $[M+Na]^+$, and the molecular formula was determined as $C_{33}H_{46}O_5$ by HR-ESI-TOF MS, respectively. The ^1H and ^{13}C NMR spectra of **1**, **2**, and **3** showed very similar signals with those of **4** except for the signals assignable to the side chain part, indicating that **1**, **2**, and **3** are geometric isomers for the side chain part of **4**, respectively (Tables 1 and 2). This presumption was supported by the detailed 2D NMR analysis (COSY, HMQC, HMBC, and NOESY).

The geometry of the 13-ene in **1** was assigned to be *Z*, since the H-15 (δ 7.99) in **1** was observed at lower field in comparison with that (δ 6.61) of **4** by the anisotropic effect of the C-12 carbonyl group. The NOESY correlations between H-18 and H-16, H-30; H-17 and H-15, H-21; H-22 and H-16, H-24; H-23 and H-21, H-26, and the coupling constants of $^3J_{15,16}$ and $^3J_{22,23}$ (each 15.1 Hz) indicated that the geometries of the conjugated penta-ene part in **1** were 13*Z*, 15*E*, 17*Z*, and 22*E*, respectively (Fig. 4a). From these data, the relative chemical structure of **1** was confirmed as shown in Figure 1.

The low field shift of the H-15 signal (δ 8.06) in **2** by the anisotropic effect of the C-12 carbonyl group also defined the 13*Z* geometry in **2**. The coupling constants of $^3J_{15,16}$ and $^3J_{22,23}$ (15.4 and 15.1 Hz, respectively) and the NOESY correlations (between H-18 and H-16, H-30; H-17 and H-15, H-22; H-21 and H-16, H-23; H-24 and H-22, H-26) revealed the geometries of the conjugated penta-ene part in **2** as 13*Z*, 15*E*, 17*E*, and 22*E* (Fig. 4b). In the same way, the chemical structure of compound **3** was confirmed by the following data ($^3J_{15,16}$ = 14.8 Hz, $^3J_{22,23}$ = 15.1 Hz, NOESY correlations: between H-15 and H-17, H-30; H-16 and H-18, H-22; H-21 and H-17, H-23; H-24 and H-22, H-26) (Fig. 4c).

The ESI-TOF MS of globostellatic acid F methyl ester (**5**) showed a quasi-molecular ion peak at *m*/*z* 579 $[M+Na]^+$, and the molecular formula was determined as $C_{33}H_{48}O_7$ by HR-ESI-TOF MS. The ^1H and ^{13}C NMR data of **5** were also very similar to those of **4**, except for the presence of the signals of an oxymethine carbon (δ 4.02, δc 79.8) and an oxygenated quaternary carbon (δc 73.1) and eight olefinic carbons. Detailed 2D NMR (COSY, HMQC, HMBC, and NOESY) analysis of **5** revealed that compound **5** has a terminal diol moiety at C-24 and C-25 in the side chain (Fig. 5). The geometries of the conjugated tetra-ene unit of the side chain in **5** were determined by the chemical shift of the H-15 (δ 6.66), the NOESY correlations, and the coupling constants ($^3J_{15,16}$ and $^3J_{22,23}$) in **5** (Fig. 5). The chemical structure of **5** was elucidated as shown in Figure 1 from the detailed 2D NMR (COSY, HMQC, HMBC, NOESY) analysis.

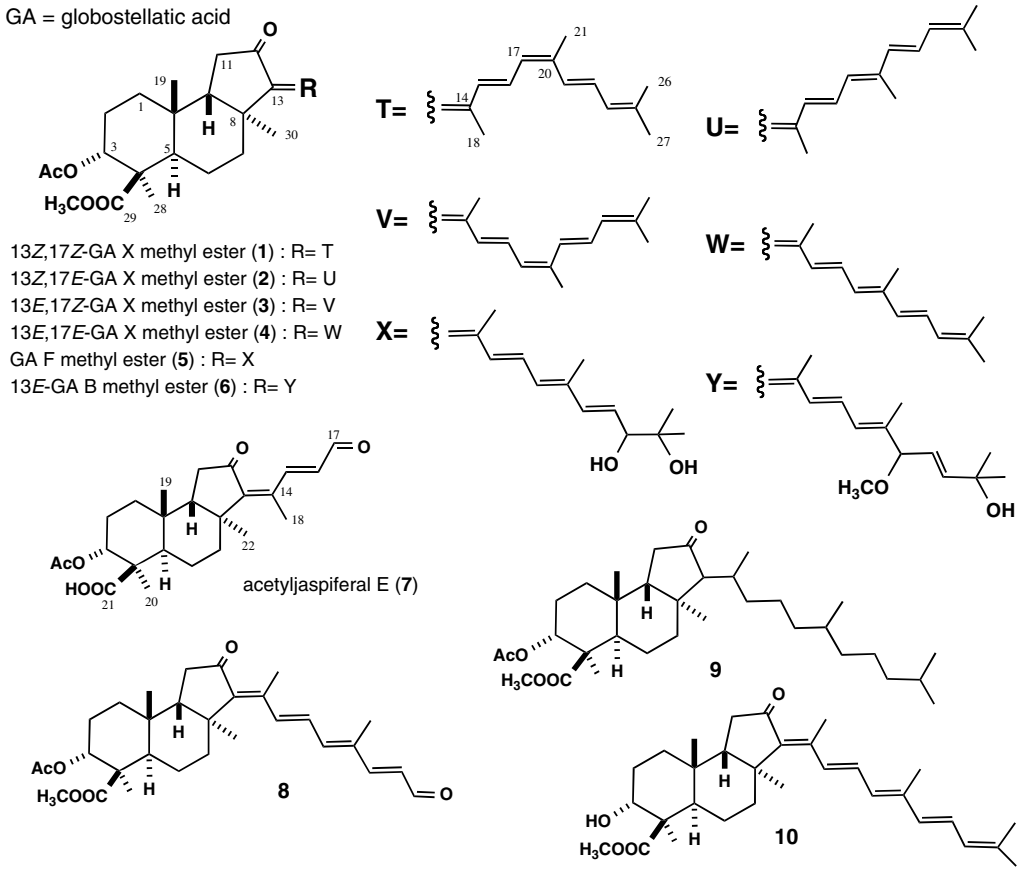

Figure 1. Chemical structures of globostellatic acid X methyl esters and the related compounds.

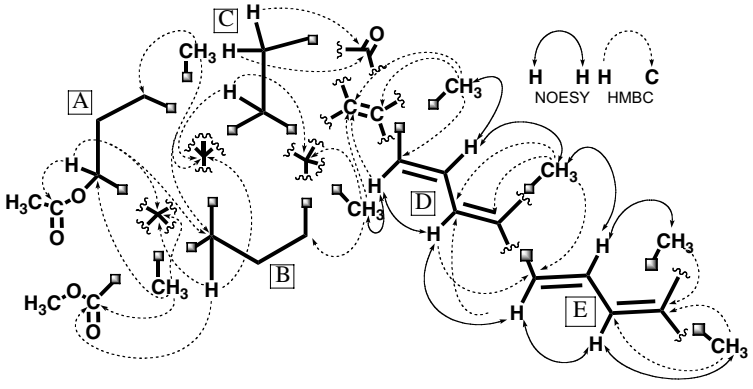

Figure 2. HMBC and NOESY correlations among partial structures of **4**.

The ESI-TOF MS of 13*E*-globostellatic acid B methyl ester (**6**) showed a quasi-molecular ion peak at *m*/*z* 593 $[M+Na]^+$, and the molecular formula was determined as $C_{34}H_{50}O_7$ by HR-ESI-TOF MS. The presence of the identical isomarabarican-type triterpene skeleton with that of **4** was also indicated by the similarity of the ^1H and ^{13}C NMR data of **6**. Compound **6** additionally showed the presence of an oxymethine (δ 4.05, δc 86.4), a methoxy group (δ 3.27 (3H, s), δc 56.0), and an oxygenated quaternary carbon (δc 70.7) together with eight olefinic carbons (Fig. 6). The chemical structure of **6** was elucidated by the detailed analysis of the 2D NMR (COSY, HMQC, HMBC, and NOESY) spectra of **6** as shown in Figure 1. Compounds **5** and **6** were named as globostellatic acid F methyl ester and 13*E*-globostellatic acid B methyl ester, respectively. Since, the related compounds named globostellatic acids A–D have been isolated from the marine sponge *Stelletta globostellata*[11]. For the scarcity of the isolated amount, the stereochemistries of the 24-hydroxyl group in **5** and the 22-methoxyl group in **6** were not investigated.

Acetyljaspiferal E (**7**) showed a quasi-molecular ion peak at *m*/*z* 439 $[M+Na]^+$, and the molecular formula was determined as $C_{24}H_{32}O_6$ by HR-ESI-TOF MS. The ^1H and ^{13}C NMR signals ascribable to the tri-cyclic

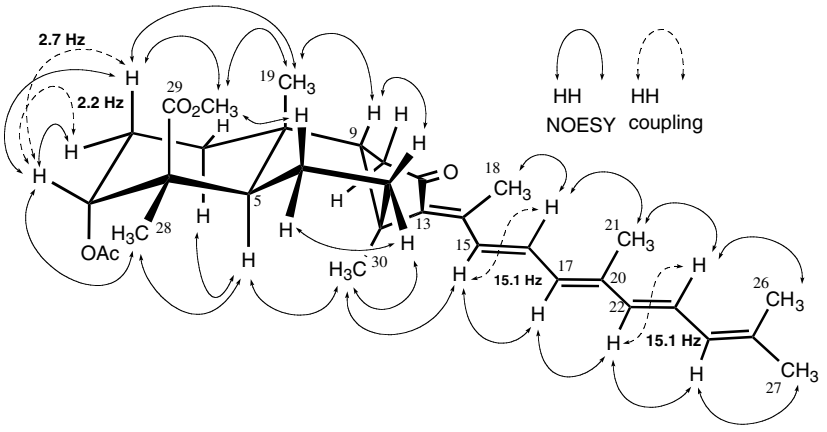

Figure 3. NOESY correlations for 13*Z*,17*Z*-globostellatic acid X methyl ester (**4**).

Table 1. ^{1}H NMR data for globostellatic acid X methyl esters

Position	δ (ppm, *J* in Hz)			
	1	**2**	**3**	**4**
1	1.76 (m)	1.74 (m)	1.75 (m)	1.75 (m)
	1.17 (m)	1.17 (m)	1.17 (m)	1.18 (m)
2	2.15 (m)	2.13 (m)	2.15 (m)	2.14 (m)
	1.77 (m)	1.75 (m)	1.77 (m)	1.76 (m)
3	5.43 (bs)	5.43 (dd, 2.7, 2.7)	5.43 (dd, 2.5, 2.7)	5.42 (dd, 2.2, 2.7)
5	2.41 (br d, 12.1)	2.41 (br d, 11.5)	2.43 (br d, 11.5)	2.43 (br d, 12.4)
6	1.90 (m)	1.90 (m)	1.88 (m)	1.88 (m)
	1.77 (m)	1.74 (m)	1.74 (m)	1.73 (m)
7	2.16 (m)	2.12 (m)	2.20 (m)	2.20 (m)
	2.10 (m)	2.10 (m)	2.18 (m)	2.17 (m)
9	1.86 (m)	1.87 (m)	1.87 (m)	1.84 (m)
11	2.22 (m)	2.22 (m)	2.22 (m)	2.22 (m)
	2.14 (m)	2.13 (m)	2.15 (m)	2.12 (m)
15	7.99 (d, 15.1)	8.06 (d, 15.4)	6.55 (d, 14.8)	6.61 (d, 15.1)
16	7.14 (dd, 15.1, 11.5)	7.00 (dd, 15.4, 11.5)	7.18 (dd, 14.8, 11.5)	7.04 (dd, 15.1, 11.3)
17	6.16 (d, 11.5)	6.29 (d, 11.5)	6.10 (d, 11.5)	6.23 (d, 11.3)
18	2.06 (3H, s)	2.05 (3H, s)	2.35 (3H, s)	2.33 (3H, s)
19	0.82 (3H, s)	0.82 (3H, s)	0.82 (3H, s)	0.81 (3H, s)
21	1.98 (3H, s)	1.97 (3H, s)	2.00 (3H, s)	2.00 (3H, s)
22	6.73 (d, 15.1)	6.24 (d, 15.1)	6.76 (d, 15.1)	6.21 (d, 15.1)
23	6.54 (dd, 15.1, 11.0)	6.53 (dd, 15.1, 11.0)	6.58 (dd, 15.1, 10.7)	6.58 (dd, 15.1, 11.0)
24	6.00 (d, 11.0)	5.95 (d, 11.0)	6.03 (d, 10.7)	5.94 (d, 11.0)
26	1.83 (3H, s)	1.82 (3H, s)	1.84 (3H, s)	1.83 (3H, s)
27	1.85 (3H, s)	1.83 (3H, s)	1.85 (3H, s)	1.84 (3H, s)
28	1.19 (3H, s)	1.18 (3H, s)	1.19 (3H, s)	1.19 (3H, s)
30	1.44 (3H, s)	1.41 (3H, s)	1.43 (3H, s)	1.43 (3H, s)
Ac	2.08 (3H, s)	2.08 (3H, s)	2.08 (3H, s)	2.08 (3H, s)
OMe	3.66 (3H, s)	3.66 (3H, s)	3.66 (3H, s)	3.65 (3H, s)

skeleton in **7** (Tables 3 and 4) were closely similar to those of **4**, and compound **7** was deduced to have the same isomarabarican-type ring structure with that of **4**. Whereas, the presence of the shorter side chain (δ 8.83, 6.39) conjugated with an aldehyde (δ 9.70, δc 195.0) was disclosed from the 2D NMR (COSY, HMQC, and HMBC) analysis. The geometries of the conjugated dienone part in **7** were confirmed as 13*Z* and 15*E* from the chemical shift (δ 8.83) of the H-15 and the $^{3}J_{15,16}$ value (15.9 Hz) (Fig. 7), and the structure of **7** was elucidated as shown in Figure 1. Consequently, compound **7** was defined to be an 3-acetyl derivative of jaspiferal E [12], which has been isolated from the marine sponge *Jaspis stellifera*.

3. Biological activity

Proliferation, migration, and tubular formation of endothelial cells are essential for angiogenesis. We first examined inhibitory effect of each compound (**1**–**10**) on the cell proliferation of HUVECs and several tumor cell lines. The activity was evaluated by IC_{50} value and Selectivity Index (SI) between HUVEC and other cell

Table 2. ^{13}C NMR data for globostellatic acid X methyl esters

Position	δc (ppm)			
	1	**2**	**3**	**4**
1	29.3	29.3	29.3	29.3
2	24.9	24.9	24.9	24.9
3	73.6	73.6	73.6	73.6
4	47.1	47.1	47.1	47.1
5	42.0	42.0	42.1	42.1
6	20.1	20.1	20.2	20.2
7	38.6	38.6	39.8	39.8
8	44.7	44.7	44.7	44.8
9	49.5	49.5	49.4	49.4
10	35.6	35.6	35.6	35.6
11	36.9	36.9	36.8	36.7
12	206.3	206.3	207.3	207.3
13	145.5	145.5	146.0	146.0
14	142.9	142.9	142.1	142.0
15	131.4	132.1	131.3	132.0
16	130.0	131.3	131.2	132.5
17	130.0	131.5	129.2	130.8
18	16.0	16.0	14.6	14.2
19	19.5	19.5	19.5	19.5
20	137.8	139.2	138.4	139.8
21	20.9	13.0	21.0	13.1
22	126.5	134.8	126.2	134.4
23	127.3	126.0	128.1	126.9
24	126.0	126.0	126.0	125.8
25	137.7	136.9	138.4	137.6
26	18.6	18.6	18.7	18.7
27	26.3	26.3	26.4	26.3
28	23.1	23.1	23.1	23.1
29	176.0	176.7	176.7	176.7
30	24.5	24.5	25.5	25.6
Ac	169.9	169.9	169.9	169.9
	21.2	21.2	21.2	21.2
OMe	51.5	51.5	51.5	51.4

lines as shown in Table 5. Among the isolated compounds, compounds **3** and **4** having 13*E* geometry exhibited both strong anti-proliferative activity and high SI value. While, compounds **1** and **2** having 13*Z* geometry showed 30–40% lower selectivity than those of **3** and **4**. Although each of globostellatic acid X was isolated as a methyl ester derivative (**1**, **2**, **3**, and **4**) by the TMS–diazomethane treatment, the mixture of the free acid form (the ratio of the free acid form of compounds **1**, **2**, **3**, and **4** is ca. 1:1:1:3) also exhibited the similar anti-proliferative activity and high SI value. On the other hand, the anti-proliferative activity against HUVECs and SI value of compounds **5**–**8** having an oxygenated side chain dramatically decreased. Compound **9** having a saturated side chain, which was obtained from **4** by Pd/C reduction, showed neither inhibitory activity of cell proliferation nor selectivity. Furthermore, the 3-hydroxyl derivative **10**, which was obtained by methanolysis of **4**, showed only weak anti-proliferative activity. These data suggested that the following three structural elements would be important for the anti-proliferative activity and high SI value; (1) unoxygenated conjugated penta-ene moiety in the side chain, (2) 3-acetyl group, and (3) 13*E* geometry.

The inhibitory effect of 13*E*,17*E*-globostellatic acid X methyl ester (**4**) on the VEGF-induced migration of

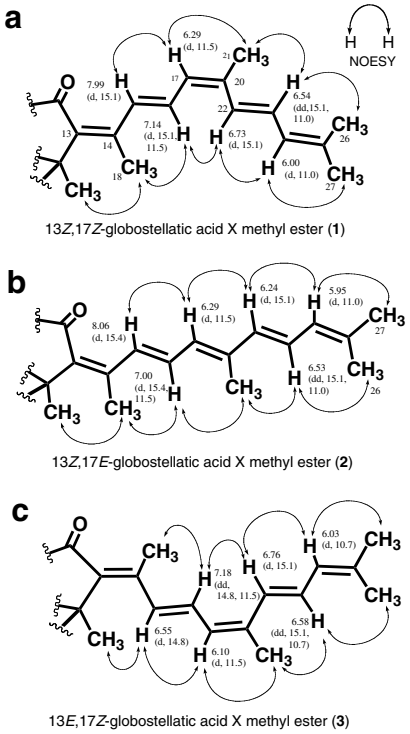

Figure 4. NOESY correlations for the conjugated penta-ene part of **1**, **2**, and **3**.

HUVECs was examined by using chemotactic chamber method. As shown in Figure 8, the 200 cells/area of HUVECs were migrated to the reverse side of the membrane filter coated with fibronectin by the stimulation of VEGF (20 ng/ml). When HUVECs were pre-incubated with 0.3 μM concentration of **4** for 12 h, the number of the migrated HUVECs decreased to 110 cells/area, and the pre-incubation with 1.0 μM of **4** inhibited the migration of HUVECs completely.

The inhibitory effect of **4** on the bFGF-induced tubular formation of HUVECs was also evaluated by the Matrigel tubular formation assay (Fig. 9). When HUVECs were plated on the Matrigel in the presence of bFGF, the cells aligned with high motility and cell–cell communication and formed a tight tubular network within 6 h. The bFGF-induced tubular formation was partly inhibited by the 12 h pre-treatment with 0.1 μM concentration of **4**, and the HUVECs pre-treated with 0.3 μM of **4** were not able to form tubular network completely.

Proliferation and migration of HUVECs requires activation of MAPK pathway induced by the growth factor such as VEGF. Transcription of genes, which relate proliferation and migration of HUVECs, is regulated by phosphorylation of ERK1/2 catalyzed by MEK1/2.[13] To analyze action-mechanism of **4**, the phosphorylation of ERK1/2 of HUVECs was examined by using Western blotting method (Fig. 10). Although 1 or 10 μM concentration of **4** exhibited more than 90% growth inhibition of HUVECs, the amount of the phosphorylated ERK1/2 of HUVECs induced by the VEGF-stimulation was not affected by the treatment with these concentrations of **4**. This result suggested that **4** inhibited proliferation

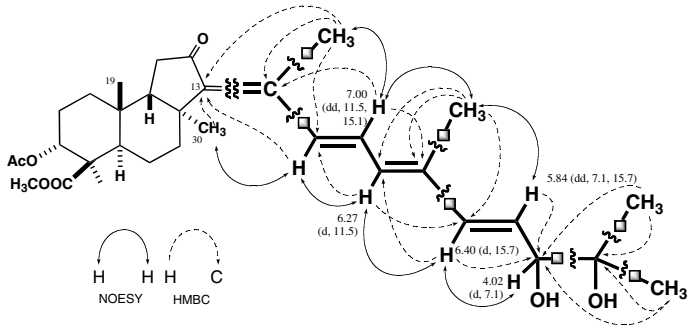

Figure 5. HMBC and NOESY correlations for the side chain part of globostellatic acid F methyl ester (**5**).

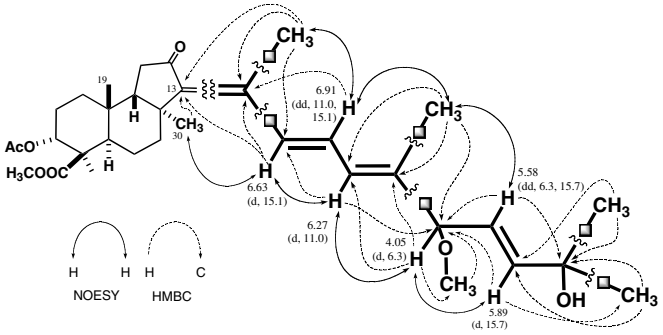

Figure 6. HMBC and NOESY correlations for the side chain part of 13*E*-globostellatic acid B methyl ester (**6**).

Table 3. ^{1}H NMR data for the related globostellatic acid methyl esters

Position	δ (ppm, J in Hz)		
	5	**6**	**7**
1	1.75 (m)	1.73 (m)	1.75 (m)
	1.19 (m)	1.16 (m)	1.22 (m)
2	2.14 (m)	2.12 (m)	2.28 (m)
	1.77 (m)	1.75 (m)	1.78 (m)
3	5.43 (dr s)	5.43 (br s)	5.41 (br s)
5	2.43 (br d, 12.3)	2.43 (br d, 12.6)	2.42 (br d, 11.3)
6	1.89 (m)	1.87 (m)	1.98 (m)
	1.76 (m)	1.74 (m)	1.84 (m)
7	2.20 (m)	2.18 (2H, m)	2.18 (2H, m)
	2.17 (m)		
9	1.87 (m)	1.85 (m)	1.95 (m)
11	2.22 (m)	2.20 (m)	2.26 (2H, m)
	2.15 (m)	2.13 (m)	
15	6.66 (d, 15.1)	6.63 (d, 15.1)	8.83 (d, 15.9)
16	7.00 (dd, 11.5, 15.1)	6.91 (dd, 11.0, 15.1)	6.39 (dd, 7.7, 15.9)
17	6.27 (d, 11.5)	6.27 (d, 11.0)	9.70 (d, 7.7)
18	2.33 (3H, s)	2.32 (3H, s)	2.05 (3H, s)
19	0.82 (3H, s)	0.82 (3H, s)	0.97 (3H, s)
20	—	—	1.27 (3H, s)
21	1.97 (3H, s)	1.78 (3H, s)	—
22	6.40 (d, 15.7)	4.05 (d, 6.3)	1.44 (3H, s)
23	5.84 (dd, 7.1, 15.7)	5.58 (dd, 6.3, 15.7)	—
24	4.02 (d, 7.1)	5.58 (d, 15.7)	
26	1.25 (3H, s)	1.34 (3H, s)	—
27	1.18 (3H, s)	1.34 (3H, s)	—
28	1.19 (3H, s)	1.19 (3H, s)	—
30	1.43 (3H, s)	1.44 (3H, s)	—
OAc	2.08 (3H, s)	2.08 (3H, s)	2.10 (3H, s)
29-OMe	3.66 (3H, s)	3.66 (3H, s)	—
22-OMe	—	3.27 (3H, s)	—

and migration of HUVECs without inhibition of ERK1/2 activation pathway.

Compound **4** induced cell death of HUVECs accompanying with morphological change (data not shown). We further investigated whether compound **4** is able to induce apoptotic cell death against HUVECs based on the activation of caspase 3/7 or not. The 5- and 17-fold increases of the caspase 3/7 activity in HUVECs were observed by the 48-h treatment with 1 and 10 μM concentrations of **4**, respectively (Fig. 11). In the case of the 60-h incubation, the activity of caspase 3/7 increased 13- and 45-fold by the treatment with 1 and 10 μM concentrations of **4**, respectively. On the other hand, the activation of caspase 3/7 of KB3-1 cells by **4** was not observed up to 10 μM concentration.

4. Experimental

4.1. Chemicals and reagents

Dulbecco's modified Eagle's medium (DMEM) and RPMI 1640 were purchased from Nissui Pharmaceutical Co. (Tokyo, Japan). WST-8 colorimetric reagent was from Nakalai Tesque, Inc. (Kyoto, Japan). The Chemotaxicell chamber (8 μm) was obtained from Kurabo Inc., (Osaka, Japan). Human recombinant $VEGF_{165}$, human recombinant bFGF were from PEPRO TECH EC LTD (LONDON, UK). A monoclonal p44/42 MAP kinase antibody and phosphor-p44/42 MAP kinase antibody were from Cell Signaling (Danvers, MA). Caspase-Glo® 3/7 Assay kit was from Promega Corp. (Madison,

Table 4. ^{13}C NMR data for the related globostellatic acid methyl esters

Position	δc (ppm)		
	5	**6**	**7**
1	29.3	29.3	29.3
2	24.9	24.9	24.9
3	73.6	73.6	73.1
4	47.1	47.1	46.9
5	42.1	42.1	42.0
6	20.2	20.1	19.9
7	39.8	39.8	38.0
8	44.8	44.7	45.0
9	49.4	49.4	49.1
10	35.6	35.6	35.9
11	36.7	36.7	36.6
12	207.4	207.5	206.4
13	146.6	146.4	151.9
14	141.5	141.6	138.6
15	133.3	132.6	150.9
16	131.8	131.5	132.5
17	132.3	127.1	195.0
18	14.5	14.4	16.0
19	19.5	19.5	19.7
20	137.7	141.0	23.2
21	13.2	13.0	180.5
22	137.2	86.4	24.9
23	128.6	125.3	—
24	79.8	140.7	—
25	73.1	70.7	—
26	26.5	29.8	—
27	23.9	29.8	—
28	23.1	23.1	—
29	176.6	176.6	—
30	25.6	25.6	—
OAc	169.9	169.9	169.8
	21.2	21.2	21.2
29-OMe	51.5	51.5	—
22-OMe	—	56.0	—

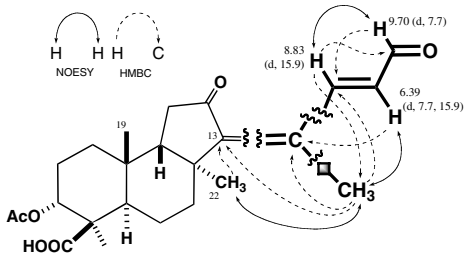

Figure 7. HMBC and NOESY correlations for the conjugated dienone part of acetyljaspiferal E (**7**).

WI). The other reagents were purchased from Sigma Chemical Co., Ltd (St. Louis, MO) or Nakalai Tesque, Inc. (Kyoto, Japan).

4.2. Isolation of globostellatic acid X methyl esters

The dried marine sponge of *R. globostellata* (1.5 kg), which was collected in July, 1999 at Sulawesi Island, Indonesia, was extracted with MeOH to obtain a MeOH extract (245 g). The MeOH extract (100 g), which exhibited selective growth inhibitory activity against HUVECs, was partitioned into a water–EtOAc mixture (1:1). The AcOEt soluble portion was further partitioned into a 90% aq MeOH–*n*-hexane mixture (1:1) to provide 90% MeOH extract (10.0 g) and *n*-hexane extract (10.0 g). On the guidance of the growth inhibition assay, the active *n*-hexane extract (10.0 g) was separated by SiO_2 column chromatography (*n*-hexane → *n*-hexane:$CHCl_3$ → $CHCl_3$:acetone → acetone → MeOH) to furnish an active fraction (Fr. 4) (856 mg). The Fr. 4 (400 mg) was further separated by HPLC (Cosmosil 5SL-II, CH_2Cl_2–MeOH) to furnish Fr. 44 (216 mg) and Fr. 45 (25 mg). The Fr. 44 was converted to the corresponding methyl esters by TMS–diazomethane (2 M hexane solution) treatment and separated by reversed-phase HPLC (Cosmosil $5C_{18}$-MS-II, CH_3CN) to afford 13*Z*,17*Z*-globostellatic acid X methyl ester (**1**, 16 mg), 13*Z*,17*E*-globostellatic acid X methyl ester (**2**, 17 mg), 13*E*,17*Z*-globostellatic acid X methyl ester (**3**, 15 mg), and 13*E*,17*E*-globostellatic acid X methyl ester (**4**, 43 mg). The Fr. 45 was purified by HPLC (Unison-UK Silica, hexane:EtOH) to furnish acetyljaspiferal E (**7**) (2 mg).

The 90% MeOH extract (7.6 g) was separated by SiO_2 column ($CHCl_3$ → $CHCl_3$:acetone → acetone → MeOH) to furnish five fractions (Fr. M1–Fr. M5). The Fr. M2 (1100 mg) was treated with TMS-diazomethane (2 M hexane solution), and the resulting methyl ester derivatives were separated by SiO_2 column (hexane:EtOAc → EtOAc → MeOH) and reversed-phase HPLC (Cosmosil $5C_{18}$-MS-II, CH_3CN:H_2O) to furnish acetyljaspiferal B methyl ester (**8**) (7 mg) and 13*E*-globostellatic acid B methyl ester (**6**) (9 mg). The Fr. M3 (401 mg) was also treated with TMS–diazomethane, and the resulting methyl esters were separated similarly to furnish globostellatic acid F methyl ester (**5**) (11 mg). 3-*O*-Acetyljaspiferal B methyl ester (**8**) was identified by comparison of the mass and NMR data with the reported data.[5]

13*Z*,17*Z*-Globostellatic acid X methyl ester (**1**): $[\alpha]_D^{20}$ −39.6 ($c = 0.3$, $CHCl_3$). IR ν_{max} (KBr) cm^{-1}: 2926, 1740, 1687, 1568, 1462 1375, 1244, 1168, 1043. UV λ_{max} (MeOH) nm (ε): 387 (47,000), 287 (10,500), 228 (12,500). ESI-MS: *m*/*z* 545 $[M+Na]^+$. High resolution ESI-MS: Calcd for $C_{33}H_{46}O_5Na$: *m*/*z* 545.3243. Found 545.3245. ^1H NMR (600 MHz, $CDCl_3$, δ), ^{13}C NMR (150 MHz, $CDCl_3$, δc) spectra: as shown in Tables 1 and 2.

13*Z*,17*E*-Globostellatic acid X methyl ester (**2**): $[\alpha]_D^{20}$ +9.9 ($c = 1.2$, $CHCl_3$). IR ν_{max} (KBr) cm^{-1}: 2957, 1739, 1688, 1639, 1556, 1452, 1375, 1244, 1170, 1043. UV λ_{max} (MeOH) nm (ε): 401 (41,800), 282 (18,900). ESI-MS: *m*/*z* 545 $[M+Na]^+$. High resolution ESI-MS: Calcd for $C_{33}H_{46}O_5Na$: *m*/*z* 545.3243. Found 545.3237. ^1H NMR (600 MHz, $CDCl_3$, δ), ^{13}C NMR (150 MHz, $CDCl_3$, δc) spectra: as shown in Tables 1 and 2.

13*E*,17*Z*-Globostellatic acid X methyl ester (**3**): $[\alpha]_D^{20}$ −201.4 ($c = 0.35$, $CHCl_3$). IR ν_{max} (KBr) cm^{-1}: 2955, 1739, 1689, 1637, 1566, 1541, 1450, 1375, 1246, 1170, 1043. UV λ_{max} (MeOH) nm (ε): 391 (38,000), 284

Table 5. Growth inhibitory activity of globostellatic acid methyl esters

Cell line	IC_{50} (μM)											
	1		**2**		**3**		**4**		**5**		**6**	
	IC_{50}	SI	IC_{50}	SI	IC_{50}	SI	IC_{50}	SI	IC_{50}	SI	IC_{50}	SI
HUVEC	0.4		0.064		0.06		0.09		0.98		1.1	
KB3-1	9.8	25	3.1	48	18	200	14	156	8.6	9	6.5	6
K562	22	55	9	141	22	360	23	256	12	12	9.3	9
Neuro2A	7.9	19	3.2	50	4.7	75	7.5	83	5.0	5	6.0	6
	7		**8**		**9**		**10**		Free acid[a]			
	IC_{50}	SI	IC_{50}	SI	IC_{50}	SI	IC_{50}	SI	IC_{50}	SI		
HUVEC	2.2		0.78		>100		0.19		0.034			
KB3-1	28	13	16	20	>100	—	4.9	25	3.4	100		
K562	32	15	7.8	10	53	—	5.2	27	8.9	261		
Neuro2A	34	14	22	28	80	—	5.9	31	6.4	188		

SI, selective index; IC_{50} against testing cells/IC_{50} against HUVECs.
[a] Free acid mixture of compounds **1**–**4**.

(12,500), 228 (11,000). ESI-MS: *m/z* 545 $[M+Na]^+$. High resolution ESI-MS: Calcd for $C_{33}H_{46}O_5Na$: *m/z* 545.3243. Found 545.3243. ^1H NMR (600 MHz, $CDCl_3$, δ), ^{13}C NMR (150 MHz, $CDCl_3$, δc) spectra: as shown in Tables 1 and 2.

13*E*,17*E* -Globostellatic acid X methyl ester (**4**): $[\alpha]_D^{20}$ −226.9 ($c = 3.2$, $CHCl_3$). IR ν_{max} (KBr) cm^{-1}: 2955, 1740, 1691, 1639, 1541 1452, 1375, 1244, 1201, 1174, 1043. UV λ_{max} (MeOH) nm (ε): 400 (47,000), 280 (10,500). ESI-MS: *m/z* 545 $[M+Na]^+$. High resolution ESI-MS: Calcd for $C_{33}H_{46}O_5Na$: *m/z* 545.3243. Found 545.3234. ^1H NMR (600 MHz, $CDCl_3$, δ), ^{13}C NMR (150 MHz, $CDCl_3$, δc) spectra: as shown in Tables 1 and 2.

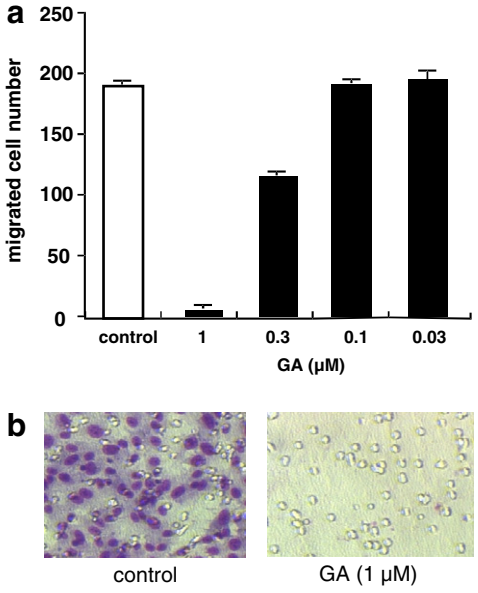

Figure 8. Effect of 13*E*,17*E*-globostellatic acid X methyl ester (**4**) on the migration of HUVECs induced by VEGF. HUVECs (1.5×10^5 cells) were treated with the indicated concentrations of **4** and stimulated with VEGF (20 ng/ml). After 6 h, the migrated cells to the reverse side of the membrane filter were counted in the six different microscopic fields. The data are presented as means ± SD (a). Representative figures of the migrated HUVECs are shown (b).

Globostellatic acid F methyl ester (**5**): $[\alpha]_D^{20}$ −176.4 ($c = 1.1$, $CHCl_3$). IR ν_{max} (KBr) cm^{-1}: 3485, 2974, 1738, 1689, 1570 1547, 1452, 1375, 1246, 1172, 1043. UV λ_{max} (MeOH) nm (ε): 369 (42,900), 253 (6000), 217 (7000). ESI-MS: *m/z* 579 $[M+Na]^+$. High resolution ESI-MS: Calcd for $C_{33}H_{48}O_7Na$: *m/z* 579.3298. Found 579.3308. ^1H NMR (600 MHz, $CDCl_3$, δ), ^{13}C NMR (150 MHz, $CDCl_3$, δc) spectra: as shown in Tables 3 and 4.

13*E*-Globostellatic acid B methyl ester (**6**): $[\alpha]_D^{20}$ −226.9 ($c = 3.2$, $CHCl_3$). IR ν_{max} (KBr) cm^{-1}: 3439, 2957, 1739, 1691, 1583, 1558, 1460, 1373, 1246, 1201, 1043. UV λ_{max} (MeOH) nm (ε): 341 (35,000), 233 (8500). ESI-MS *m/z*: 593 $[M+Na]^+$. High resolution ESI-MS: Calcd for $C_{34}H_{50}O_7Na$: *m/z* 593.3454. Found 593.3442. ^1H NMR (600 MHz, $CDCl_3$, δ), ^{13}C NMR (150 MHz, $CDCl_3$, δc) spectra: as shown in Tables 3 and 4.

Acetyljaspiferal E (**7**): $[\alpha]_D^{20}$ −72.1 ($c = 0.18$, $CHCl_3$). IR ν_{max} (KBr) cm^{-1}: 2926, 1738, 1703, 1682, 1572, 1462, 1377, 1263, 1201, 1170, 1113, 1022. UV λ_{max} (MeOH) nm (ε): 354 (5600), 303 (15,100). ESI-MS: *m/z* 439 $[M+Na]^+$. High resolution ESI-MS: Calcd for $C_{24}H_{32}O_6Na$: *m/z* 439.2097. Found 439.2107. ^1H NMR (600 MHz, $CDCl_3$, δ), ^{13}C NMR (150 MHz, $CDCl_3$, δc) spectra: as shown in Tables 3 and 4.

4.3. Reduction of 13*E*,17*E*-globostellatic acid X methyl ester (4)

A solution of **4** in MeOH (6 mg/1 ml) was treated with 10% Pd/C (2 mg) and stirred for 45 min under H_2 atmosphere. The reaction mixture was filtered and concentrated under reduced pressure. The resulting residue was purified by SiO_2 column (hexane:EtOAc) to give **9** (1.6 mg).

Compound **9**: ESI-MS: *m/z* 555 $[M+Na]^+$. High resolution ESI-MS: Calcd for $C_{33}H_{56}O_5Na$: *m/z* 555.4025. Found 555.4025.

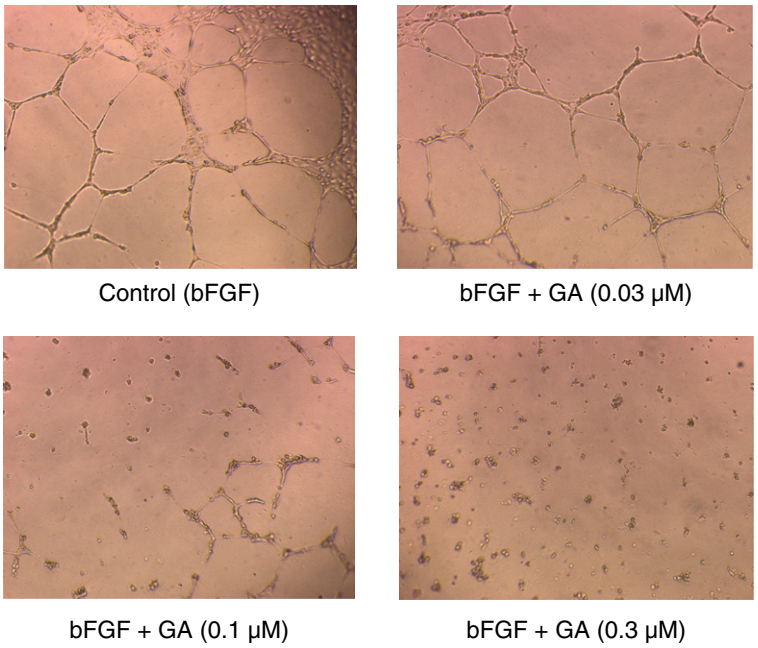

Figure 9. Effect of 13*E*,17*E*-globostellatic acid X methyl ester (**4**) on the tube formation of HUVECs induced by bFGF. HUVECs (1.0×10^4 cells) were pre-treated with the indicated concentrations of **4** for 12 h. Then, the cells were suspended in essential minimal medium supplemented with bFGF (30 ng/ml) and inoculated onto the solidified Matrigel in 96-well plates. After 10 h, images were captured under a microscope.

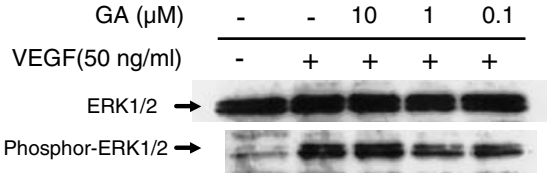

Figure 10. Effect of 13*E*,17*E*-globostellatic acid X methyl ester (**4**) on the phosphorylation of ERK1/2. HUVECs were pre-incubated with the indicated concentrations of **4** for 6 h, and then the cells were stimulated with or without VEGF (50 ng/ml) for 15 min. The cell lysate was resolved by SDS–PAGE and detected by anti-ERK1/2 antibody and anti-phosphor-ERK1/2 antibody.

4.4. Hydrolysis of 13*E*,17*E*-globostellatic acid X methyl ester (4)

Compound **4** (5 mg) was treated with 1N KOH/MeOH (500 μl) for 9 h. Reaction mixture was neutralized with 5% HCl and extracted with EtOAc to give the crude product. The crude product was purified by HPLC (Cosmosil 5SL-II, hexane:EtOAc) to give **10** (1.4 mg).

Compound **10**: $[\alpha]_D^{20}$ −56.5 ($c = 0.12$, $CHCl_3$). ESI-MS: *m/z* 503 $[M+Na]^+$. High resolution ESI-MS: Calcd for $C_{31}H_{44}O_4Na$: *m/z* 503.3137. Found 503.3110. ^1H NMR (500 MHz, $CDCl_3$, δ): 7.03 (1H, dd, $J = 11.5$, 15.3 Hz), 6.61 (1H, d, $J = 15.3$ Hz), 6.58 (1H, dd, $J = 11.0$, 15.3 Hz), 6.24 (1H, d, $J = 11.5$ Hz), 6.23 (1H, d, $J = 15.3$ Hz), 5.95 (1H, d, $J = 11.0$ Hz), 4.21 (1H, br s), 3.64 (3H, s), 2.49 (1H, br d, $J = 11.6$ Hz), 2.33 (3H, s), 2.23 (1H, m), 2.18 (1H, m), 2.17 (1H, m), 2.16 (1H, m), 2.13 (1H, m), 2.00 (3H, s), 1.86 (2H, m), 1.84 (3H, s), 1.84 (3H, s), 1.74 (1H, m), 1.71 (1H, m), 1.68 (1H, m), 1.44 (3H, s), 1.29 (3H, m), 1.13 (1H, m), 0.80 (3H, s).

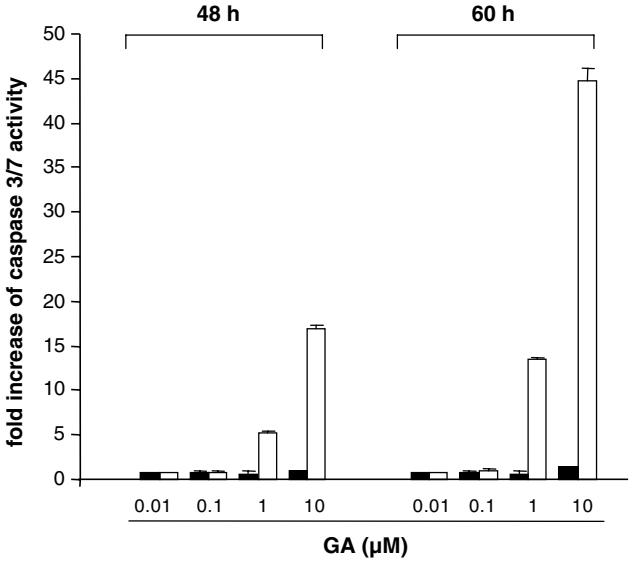

Figure 11. Caspase 3/7 activity of HUVECs and KB3-1 cells treated with 13*E*,17*E*-globostellatic acid X methyl ester (**4**). HUVECs (white bar) and KB3-1 cells (black bar) were treated with the indicated concentrations of **4** for 48 and 60 h, respectively. The caspase 3/7 activity was measured by the Caspase-Glo 3/7 assay kit.

4.5. Cell culture

HUVECs (5×10^5 cells/vial) were purchased from Kurabo Inc. and grown in HuMedia-EG2 medium with growth supplements (Kurabo Inc.). Human KB epidermoid carcinoma cells (KB3-1) were cultured in RPMI 1640 medium supplemented with heat-inactivated 10% fetal bovine serum (FBS) and kanamycin (50 μg/ml). Human chronic myelogenous leukemia cells (K562)

and murine neuroblastoma cells (Neuro2A) were cultured in RPMI 1640 medium or in Dulbecco's modified Eagle's medium (DMEM), respectively, supplemented with 10% fetal bovine serum (FBS) and kanamycin (50 μg/ml) in a humidified atmosphere of 5% CO_2 at 37 °C.

4.6. Growth inhibition assay

Each suspension of HUVECs or other cell lines in the culture medium was plated into each well of 96-well plates (2×10^3 cells/well/100 μl). After 24 h, test compounds were added, and then the plates were incubated for an additional 72 h in a humidified atmosphere of 5% CO_2 at 37 °C. The cell proliferation was detected by WST-8 colorimetric reagent. The IC_{50} value was determined by linear interpolation from the growth inhibition curve. We assessed selectivity of the anti-proliferative activity (Selective Index, SI) from the differences of IC_{50} values against HUVECs and other cell lines.

4.7. VEGF-induced migration assay

A polycarbonate filter of the inner chamber (Chemotaxicell chamber, 8 μm) was soaked in fibronectin solution (1.33 μg/ml) for 1 h at 37 °C and dried in vacuo. HUVECs were treated with different concentrations of compound **4** in serum- and growth factor-starved medium for 12 h. Then HUVECs (1.5×10^4 cells) were suspended in HuMedia-EB2 medium containing 0.2% FBS and seeded in the inner chamber. The inner chamber was put into the outer chamber (24-well plate), which was filled with the same medium containing VEGF (20 ng/ml). After 6-h incubation at 37 °C, the non-migrated cells on the upper surface of the filter were removed by wiping with cotton swabs, and the filter was fixed with 70% EtOH and stained with Giemsa. The cells, which migrated through the filter to the reverse side, were counted manually at six different areas under a microscope (×200).

4.8. VEGF-induced matrigel tubular formation assay

HUVECs were treated with the different concentrations of compound **4** in serum- and growth factor-starved medium for 12 h. 96-Well plates were coated with 50 μl of Matrigel (11.55 mg/ml) and incubated at 37 °C for 1 h to promote gelation. The HUVECs were trypsinized, washed with Hepes buffer, counted, and resuspended in HuMedia-EB2 medium supplemented with bFGF (30 ng/ml) and 0.2% FBS. Then, the HUVECs (1×10^4 cells/well) were seeded onto the solidified Matrigel in 96-well plates. The plates were incubated in a humidified atmosphere of 5% CO_2 at 37 °C. After 10 h, tubular network patterns were captured through an inverted phase contrast microscope and photographed.

4.9. Immunoblotting assay

HUVECs were cultured in Petri dish with serum- and growth factor- (bFGF and EGF) starved HuMedia-EG2 medium for 24 h. The confluent cells were then pre-incubated with the indicated concentrations of compound **4** for 6 h and stimulated with VEGF (50 ng/ml) for 15 min at 37 °C. The cells were rinsed with ice-cold PBS and lysed in lysis buffer (50 mM Tris–HCl (pH 8.0), 137 mM NaCl, 200 mM EDTA, 1% Triton X-100, and 10% glycerol containing 1 mM phenylmethylsulfonyl fluoride (PMSF), 1% protease inhibitor cocktail-DMSO solution, and 1 mM sodium vanadate). The cell lysate was subjected to SDS–PAGE and transferred onto PVDF membranes (Amersham, UK). The membrane was incubated with the blocking solution and probed with the primary antibodies (anti-p44/42 MAP kinase antibody and anti-phosphor-p44/42 MAP kinase antibody). Immunoreactive proteins were visualized by enhanced chemiluminescence (Amersham, UK).

4.10. Assay for caspase-3/7 activity

HUVECs and KB 3-1 cells (2×10^3 cells/well) were inoculated into 96-well plates. After 24 h, test compounds were added and the plates were incubated for the indicated time in a humidified atmosphere of 5% CO_2 at 37 °C. A caspase luminescent assay (Promega Corp., Madison, WI) was used to determine enzymatic activity of caspase 3/7 according to the manufacturer's instructions. Cleavage of the proluminescent substrate (z-DEVD-aminoluciferin) containing DEVD sequence by caspase 3/7 was monitored by a luminometer (Berthold Technologies, Bad Wildbad, Germany). Quantification of caspase 3/7 was corrected by the number of living cells measured by WST8 growth inhibition assay, and caspase 3/7 activity was calculated as fold increase over the control.

Acknowledgments

The authors are grateful to Dr. Nicole J. de Voogd, National Museum of Natural History, the Netherlands, for identification of the sponge. This study was financially supported by Grant-in-Aid for scientific research from the Ministry of Education, Culture, Sports, Science and Technology of Japan.

References and notes

1. Folkman, J. *Nat. Med.* **1995**, *1*, 27.
2. Folkman, J.; Shing, Y. *J. Biol. Chem.* **1992**, *267*, 10931.
3. Folkman, J.; Merler, E.; Abernathy, C.; Williams, G. *J. Exp. Med.* **1971**, *133*, 275.
4. Aoki, S.; Cho, S. H.; Ono, M.; Kuwano, T.; Nakao, S.; Kuwano, M.; Nakagawa, S.; Gao, J. Q.; Mayumi, T.; Shibuya, M.; Kobayashi, M. *Anticancer Drugs* **2006**, *17*, 269.
5. Zampella, A.; D'Auria, M. V.; Debitus, C.; Menou, J. L. *J. Nat. Prod.* **2000**, *63*, 943.
6. McCormick, J. L.; McKee, T. C.; Cardellina, J. H.; Leid, M.; Boyd, M. R. *J. Nat. Prod.* **1996**, *59*, 1047.
7. Tasdemir, D.; Mangalindan, G. C.; Concepcion, G. P.; Verbitski, S. M.; Rabindran, S.; Miranda, M.; Greenstein, M.; Hooper, J. N.; Harper, M. K.; Ireland, C. M. *J. Nat. Prod.* **2002**, *65*, 210.

8. Kondracki, M. L. B.; Longeon, A.; Debitus, C.; Guyot, M. *Tetrahedron Lett.* **2000**, *41*, 3087.
9. Rao, Z.; Deng, S.; Wu, H.; Jiang, S. *J. Nat. Prod.* **1997**, *60*, 1163.
10. Tsuda, M.; Ishibashi, M.; Agemi, K.; Sasaki, T.; Kobayashi, J. *Tetrahedron* **1991**, *47*, 2181.
11. Ryu, G.; Matsunaga, S.; Fusetani, N. *J. Nat. Prod.* **1996**, *59*, 512.
12. Kobayashi, J.; Yuasa, K.; Kobayashi, T.; Sasaki, T.; Tsuda, M. *Tetrahedron* **1996**, *52*, 5745.
13. Hood, J. D.; Frausto, R.; Kiosses, W. B.; Schwartz, M. A.; Cheresh, D. A. *J. Cell Biol.* **2003**, *162*, 933.